

AD-A100 340

DETECTION OF EXCITED STATES BY LASER-INDUCED
FLUORESCENCE(U) NATIONAL BUREAU OF STANDARDS BOULDER CO
QUANTUM PHYSICS DIV A B WEDDING ET AL. APR 87

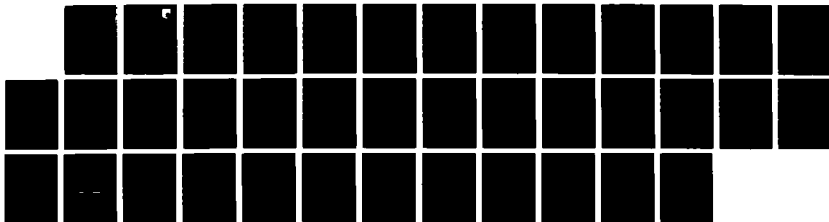
1/1

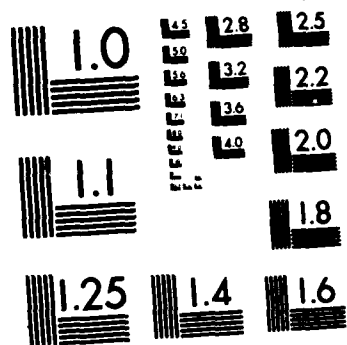
UNCLASSIFIED

AFMNL-TR-86-2113 MIPR-FV1455-85-0601

F/G 20/5

NL





MICROCOPY RESOLUTION TEST CHART
NATIONAL BUREAU OF STANDARDS-1963-A

DTIC FILE COPY

AD-A180 348

AFWAL-TR-86-2113



DETECTION OF EXCITED STATES BY LASER-INDUCED FLUORESCENCE

A. B. WEDDING and A. V. PHELPS

QUANTUM PHYSICS DIVISION
U. S. BUREAU OF STANDARDS
BOULDER, CO 80303

April 1987

FINAL REPORT FOR PERIOD OCTOBER 1982 - SEPTEMBER 1986

Approved for public release; distribution is unlimited

AERO PROPULSION LABORATORY
AIR FORCE WRIGHT AERONAUTICAL LABORATORIES
AIR FORCE SYSTEMS COMMAND
WRIGHT-PATTERSON AIR FORCE BASE, OHIO 45433-6563

87 5 21 007

NOTICE

When Government drawings, specifications, or other data are used for any purpose other than in connection with a definitely related Government procurement operation, the United States Government thereby incurs no responsibility nor any obligation whatsoever; and the fact that the Government may have formulated, furnished, or in any way supplied the said drawings, specifications, or other data, is not to be regarded by implication or otherwise as in any manner licensing the holder or any other person or corporation, or conveying any rights or permission to manufacture, use, or sell any patented invention that may in any way be related thereto.

This report has been reviewed by the Information Office and is releasable to the National Technical Information Service (NTIS). At NTIS, it will be available to the general public, including foreign nations.

This technical report has been reviewed and is approved for publication.



ALAN GARSCADDEN
Research Physicist
Advanced Plasma Research Group
Power Components Branch
Aerospace Power Division
Aero Propulsion Laboratory
FOR THE COMMANDER



PAUL R. BERTHEAUD, Chief
Power Components Branch
Aerospace Power Division
Aero Propulsion Laboratory



JAMES D. REAMS
Chief, Aerospace Power Division
Aero Propulsion Laboratory

"If your address has changed, if you wish to be removed from our mailing list, or if the addressee is no longer employed by your organization please notify AFWAL/POOC, WPAFB, OH 45433-6563 to help us maintain a current mailing list."

Copies of this report should not be returned unless return is required by security considerations, contractual obligations, or notice on a specific document.

Unclassified

SECURITY CLASSIFICATION OF THIS PAGE

AD A 180 348

REPORT DOCUMENTATION PAGE

1a REPORT SECURITY CLASSIFICATION Unclassified			1b RESTRICTIVE MARKINGS		
2a SECURITY CLASSIFICATION AUTHORITY			3 DISTRIBUTION/AVAILABILITY OF REPORT Approved for public release; distribution is unlimited		
2b DECLASSIFICATION/DOWNGRADING SCHEDULE					
4. PERFORMING ORGANIZATION REPORT NUMBER(S)			5. MONITORING ORGANIZATION REPORT NUMBER(S) AFWAL-TR-86-2113		
6a. NAME OF PERFORMING ORGANIZATION Quantum Physics Division U.S. Bureau of Standards		6b OFFICE SYMBOL (If applicable)	7a NAME OF MONITORING ORGANIZATION Air Force Wright Aeronautical Laboratories Aeropropulsion Laboratory (AFWAL/POOC)		
6c. ADDRESS (City, State, and ZIP Code) Boulder, CO 80303			7b ADDRESS (City, State, and ZIP Code) Wright-Patterson AFB, OH 45433-6563		
8a. NAME OF FUNDING / SPONSORING ORGANIZATION		8b. OFFICE SYMBOL (If applicable)	9. PROCUREMENT INSTRUMENT IDENTIFICATION NUMBER MIPR FY 1455-85-0601		
8c. ADDRESS (City, State, and ZIP Code)			10. SOURCE OF FUNDING NUMBERS		
			PROGRAM ELEMENT NO 61102F	PROJECT NO 2301	TASK NO 51
			WORK UNIT ACCESSION NO. 24		
11 TITLE (Include Security Classification) Detection of excited states by laser-induced fluorescence (unclassified)					
12 PERSONAL AUTHOR(S) A. B. Wedding and A. V. Phelps					
13a TYPE OF REPORT Final		13b. TIME COVERED FROM Oct '82 TO Sep '86		14. DATE OF REPORT (Year, Month, Day) 1987 April	
15 PAGE COUNT 39					
16 SUPPLEMENTARY NOTATION					
17 COSATI CODES			18 SUBJECT TERMS (Continue on reverse if necessary and identify by block number)		
FIELD	GROUP	SUB GROUP			
20	6	19	hydrogen, oxygen, argon, metastables, electrons, radiation, excitation coefficient, excited states		
20	9	4			
19 ABSTRACT (Continue on reverse if necessary and identify by block number) <p>laser absorption techniques have been used to measure the collisional quenching rate coefficients for a number of levels of the H_2 state. These rate coefficients are nearly independent of rotational and vibrational quantum number, i.e., 1.7 to $2.0 \times 10^{-15} \text{ m}^3/\text{s}$. Techniques are being developed for the measurement of electron excitation coefficients for the H_2^+ state. Results are presented from attempts to model experimental measurements of 634 nm emission produced in collisions of pairs of O_2 metastables in the afterglow of pulsed discharges in O_2 mixtures.</p> <p>hydrogen oxygen argon to the negative system</p>					
20 DISTRIBUTION/AVAILABILITY OF ABSTRACT <input checked="" type="checkbox"/> UNCLASSIFIED/UNLIMITED <input type="checkbox"/> SAME AS RPT <input type="checkbox"/> DTIC USERS			21 ABSTRACT SECURITY CLASSIFICATION Unclassified		
22a NAME OF RESPONSIBLE INDIVIDUAL A. Garscadden			22b TELEPHONE (Include Area Code) (513) 255-2923		22c OFFICE SYMBOL AFWAL/POOC

DD FORM 1473, 84 MAR

83 APR edition may be used until exhausted
All other editions are obsoleteSECURITY CLASSIFICATION OF THIS PAGE
Unclassified

PREFACE

This work was performed in the Quantum Physics Division, U.S. Bureau of Standards, at the Joint Institute for Laboratory Astrophysics under MIPR FY1455-85-0601. The work was performed during the period October 1985 through September 1986 under Project 2301 Task S1, Work Unit 24. The Air Force contract manager was Dr. Alan Garscadden, Power Components Branch, Air Force Wright Aeronautical Laboratories, Aero Propulsion Laboratory, WPAFB, OH 45433-6563.



A-1

TABLE OF CONTENTS

SECTION	PAGE
I. INTRODUCTION	1
II. H_2 METASTABLE DESTRUCTION	3
III. H_2 METASTABLE EXCITATION BY ELECTRONS	15
IV. MODELS OF O_2 ($a^1\Delta_g$) IN DISCHARGES	21
V. CONCLUSIONS	27
REFERENCES	29

LIST OF ILLUSTRATIONS

FIGURE	PAGE
1. Lower rotational and vibrational levels of the $c^3\Pi_u$ and $a^3\Sigma_g^+$ states of H_2 . The levels marked with an asterisk are the levels investigated in these experiments.	4
2. Schematic of apparatus used in absorption measurements.	5
3. Upper trace: overall transient absorption waveform showing metastable increase during discharge pulse and depletion caused by pulsed laser. Lower trace: expanded absorption waveform showing recovery of $c^3\Pi_u$ ($N=1$, $v=0$) metastable population and exponential fit to data.	6
4. Measured and calculated reciprocal decay constants for $v = 0$, $N = 1$ levels of the $H_2(c^3\Pi_u)$ state vs discharge current for various pressures.	8
5. Measured destruction rate coefficients vs vibrational quantum number for $N = 1$ levels of $H_2(c^3\Pi_u)$ state.	9
6. Measured destruction rate coefficients vs rotational quantum number for $v = 1$ levels of $H_2(c^3\Pi_u)$ state.	10
7. Absorption transients for $v = 1$, $N = 1$ level (top) and $v = 0$, $N = 1$ level (bottom) of $a^3\Sigma_g^+$ state resulting from laser induced depletion of the corresponding levels of the $c^3\Pi_u$ state.	13
8. Representative current, probe voltages, emission and absorption traces for discharges in H_2	17

LIST OF ILLUSTRATIONS (Concluded)

Figure	Page
9. Electric field to gas density ratio E/n for pulsed discharges in H_2 . The solid points are our experimental data, while the + and x are those of Breusova and of Güntherschulze, respectively. The line is calculated from ambipolar diffusion theory and theoretical ionization coefficients.	18
10. Absorption line profile for the $H_2(c^3\Pi_u, v = 1, N = 1)$ to $i^3\Pi_g, v = 1, N = 1$ transition at 588.8 nm for a pulsed discharge in H_2 at 1 A current and 1 torr pressure of H_2	20
11. Electron dissociation, ionization, and metastable excitation coefficients for 33% O_2 in Ar vs E/n as calculated from our revised electron cross section sets.	23
12. Comparison of measured relative 634 nm emission data with the calculated square of the $O_2(a^1\Delta_g)$ density for a 33% $O_2 = 67\%$ Ar mixture. The solid curve is taken from the experimental data of Vasileva <u>et al.</u> , while the dashed curves are from the model discussed in the text.	25

LIST OF TABLES

TABLE	PAGE
1. Measured rate coefficients for collisional destruction of vibrational and rotational levels of $H_2(c^3\Pi_u)$ metastables.	11
2. Levels examined in search for collisional coupling between $c^3\Pi_u$ and $a^3\Sigma_g^+$ states of H_2	12
3. Rate coefficients used in model of $O_2(a^1\Delta_g)$ behavior in O_2 -Ar discharges and afterglow.	24

SECTION I

INTRODUCTION

The overall objective of the research described in this final report is to develop diagnostics and models required for measurement and prediction of the properties of electrical discharges in molecular gases. Such discharges are important to the Air Force because of their use in devices such as high power switches, negative ion sources and plasma processors and because of their role in phenomena such as lightning and corona. The research program includes; a) the development and application of laser fluorescence and absorption techniques to the measurement of excited state densities in electric discharges, b) the measurement of the properties of the excited states of importance in molecular discharges of current interest, c) the application of various diagnostic techniques to the determination of the characteristics of moderate current density, transient electrical discharges, and d) the quantitative comparison of these results with appropriate discharge models.

During the past year we have (a) completed measurements of the collisional destruction of metastable H_2 molecules in various rotational and vibrational states, (b) initiated measurements of excitation coefficients for $H_2(c^3\Pi_u)$ metastable molecules by discharge electrons, and c) attempted to model experimental determinations of the time dependence of $O_2(a^1\Delta_g)$ metastable densities in pulsed electrical discharges. The properties of metastable H_2 are of current interest because of the use of discharges in H_2 as switching devices (thyratrons), as negative ion sources, and as infrared lasers. The behavior of $O_2(^1\Delta_g)$ metastables in electric discharges is of interest because of the possibility of discharge lasers utilizing excitation

transfer from the O_2 metastable to I atoms which can undergo stimulated emission in the near infrared.

The results of work on the $c^3\Pi_u$ state of H_2 is summarized in Sec. II. The diagnostic techniques and some initial results connected with the measurement of electron excitation coefficients for the $H_2(c^3\Pi_u)$ state are discussed in Sec. III. The results obtained thus far in the analysis of the transient O_2 densities in pulsed discharges are discussed in Sec. IV. Recommendations for future work are made in Sec. V.

SECTION II

H₂ METASTABLE DESTRUCTION

In this section we summarize our measurements of rate coefficients for the destruction of various rotational and vibrational levels of the $c^3\Pi_u$ metastable state of H₂ in collisions with H₂. We also summarize a brief search for collisional coupling between H₂($c^3\Pi_u$) levels and nearby $a^3\Sigma_g^+$ levels. The experimental technique and the results for the N = 1 rotational level the v = 2 vibrational state have been published.¹ We will therefore only briefly review the experimental technique before presenting the results.

The lower rotational and vibrational levels of the $c^3\Pi_u$ state and of the nearby $a^3\Sigma_g^+$ state of H₂ are shown in Fig. 1. The levels investigated in this work are marked with an asterisk. As described in Ref. 1, the relative excited state densities were measured by observing the absorption of radiation in transitions to the $g^3\Sigma_g^+$, $i^3\Pi_g$ and $j^3\Delta_g$ states. Figure 2 shows the experimental arrangement and Fig. 3 shows a representative absorption transient. As in our previous experiments, the metastable density was suddenly reduced by exciting a large fraction of the metastables to a higher state from which a significant fraction could radiate to the $b^3\Sigma_u^+$ state and then dissociate. The time constant of the recovery of metastable population was determined by fitting an exponential to the absorption waveform during the recovery period as shown in the expanded portion of the absorption transient shown in the lower part of Fig. 3. The principal changes in the experimental apparatus are the use of a balanced detection system so as to reduce the effects of intensity fluctuations in the output of the cw dye laser source used for the absorption measurements and the replacement of the N₂-pump laser

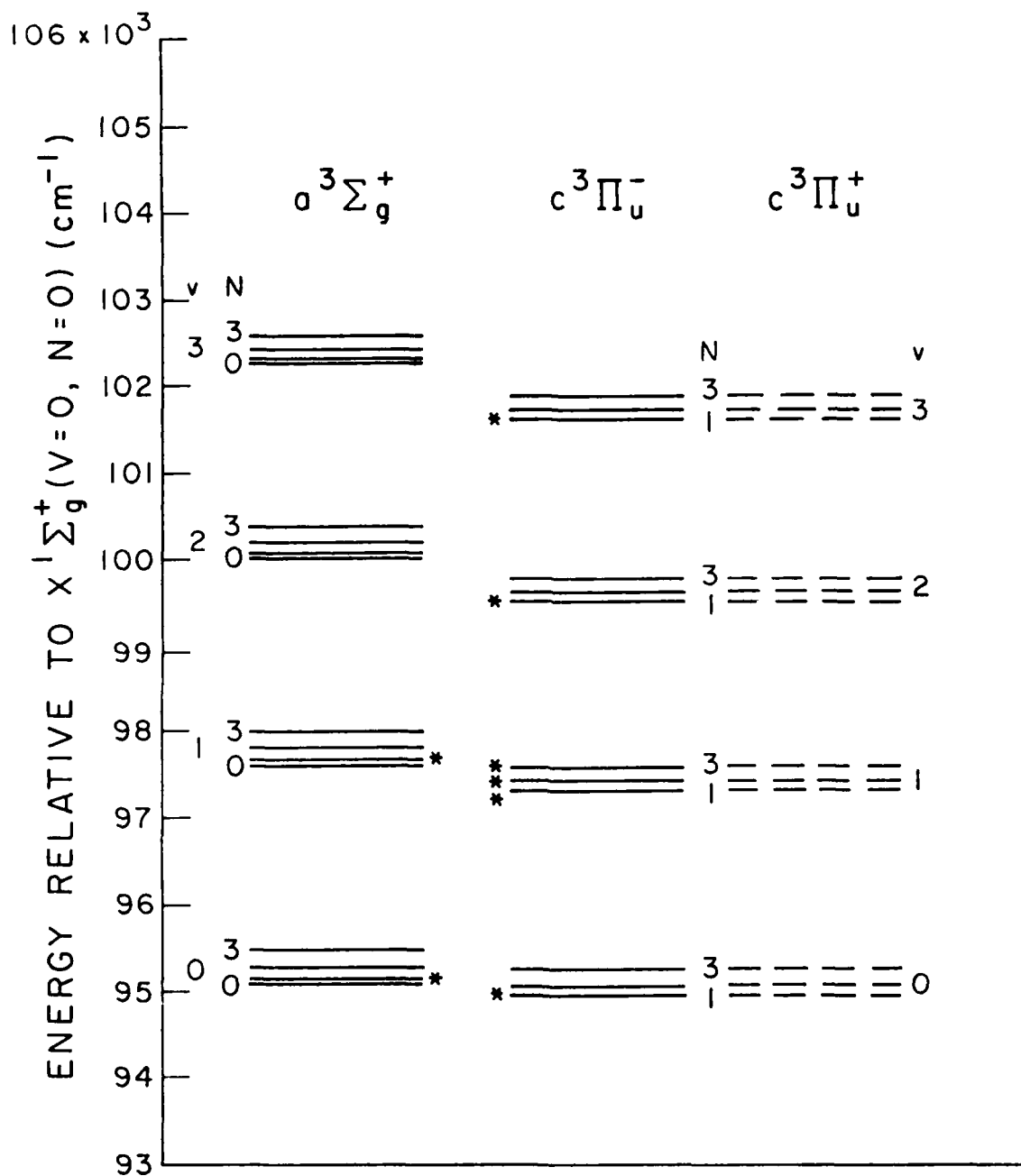


Figure 1. Lower rotational and vibrational levels of the $c^3\Pi_u$ and $a^3\Sigma_g^+$ states of H_2 . The levels marked with an asterisk are the levels investigated in these experiments.

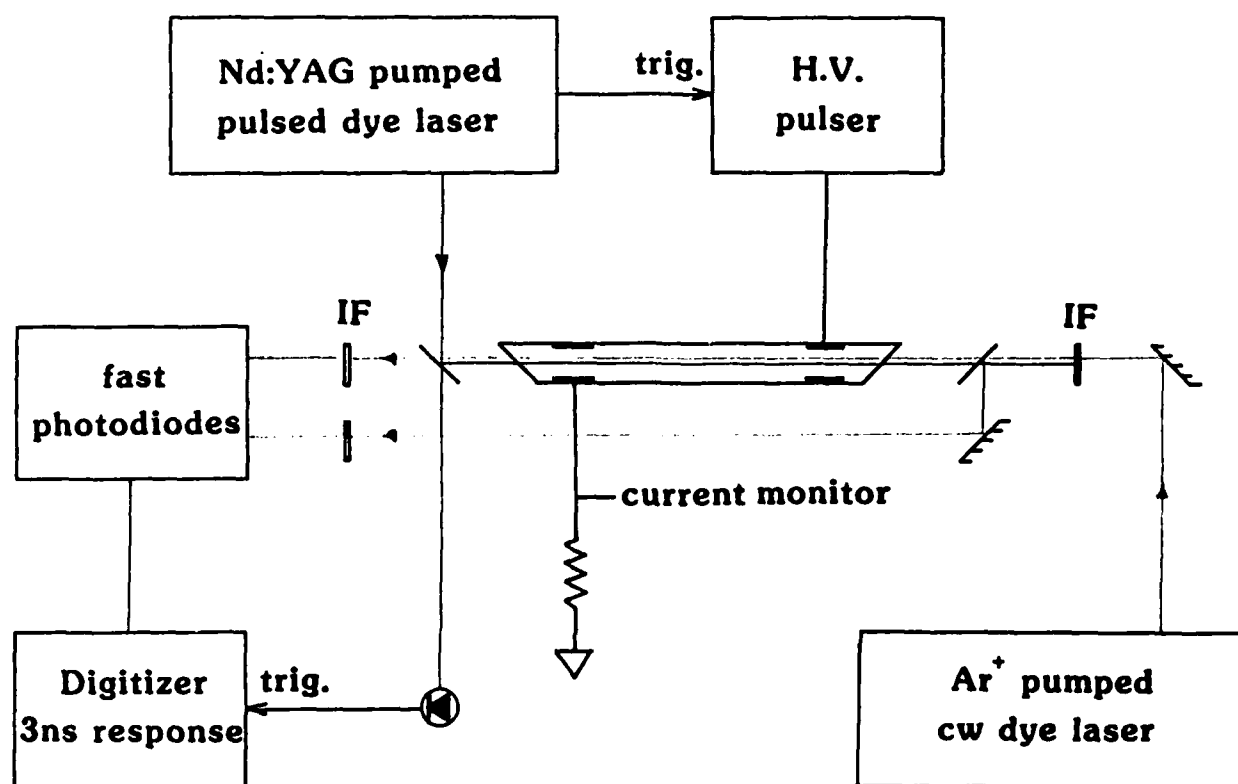


Figure 2. Schematic of apparatus used in absorption measurements.

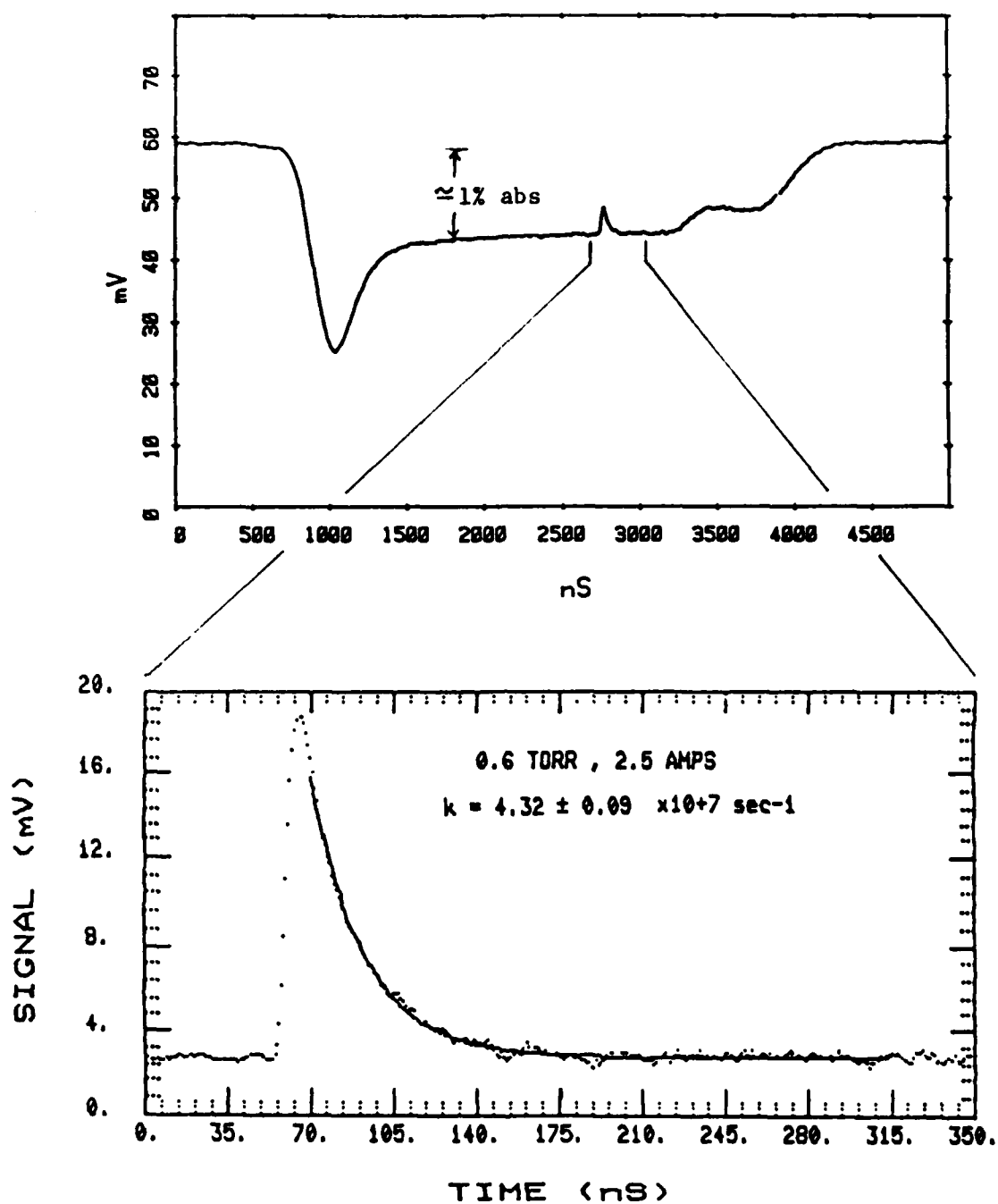


Figure 3. Upper trace: overall transient absorption waveform showing metastable increase during discharge pulse and depletion caused by pulsed laser. Lower trace: expanded absorption waveform showing recovery of $c^3\Pi_u$ ($N=1$, $v=0$) metastable population and exponential fit to data.

for the pulsed dye laser with a much more powerful and reliable Nd:YAG pump laser.

Representative rate coefficient data for the $N = 1, v = 0$ level are plotted in Fig. 4 as a function of current for various discharge pressures. The straight lines are a least squares fit to the data assuming a linear dependence of the metastable destruction on the discharge current and on the H_2 density. The rate coefficients for $H_2(c^3\Pi_u)$ destruction at zero discharge current are plotted as a function of vibrational quantum number v for $N = 1$ in Fig. 5 and as a function of rotational quantum number for $v = 1$ in Fig. 6. The error bars are indicative of the uncertainty in the average values at a given current and pressure. The results of these experiments are also tabulated in Table I. The present results for the $v = 2, N = 1$ level are in very good agreement with our published results.¹ We note that there is very little, if any, change in the destruction rate coefficient with vibrational quantum number and only about a 10% change with rotational quantum number. In view of the very large magnitude of these quenching rate coefficients and associated cross section ($\sim 80 \text{ \AA}^2$), each gas kinetic collision results in quenching and we do not expect much change with initial level.

A brief effort was made to determine whether the collisional quenching of the $c^3\Pi_u$ levels resulted in excitation transfer collisions with nearby $a^3\Sigma_g^+$ levels. In these experiments the population of one of the more highly absorbing levels of the $c^3\Pi_u$ state was perturbed by the pulsed laser and the resulting change in the $a^3\Sigma_g^+$ level density was observed by tuning the cw laser to the appropriate $a^3\Sigma_g^+$ to $d^3\Pi_u$ transition. Table II shows the combinations of $c^3\Pi_u$ and $a^3\Sigma_g^+$ levels observed, the absorption line used, and whether or not the $a^3\Sigma_g^+$ population was observed to decrease. Figure 7 shows the observed decreases in absorption for the $v = 1, N = 1$ level and for the

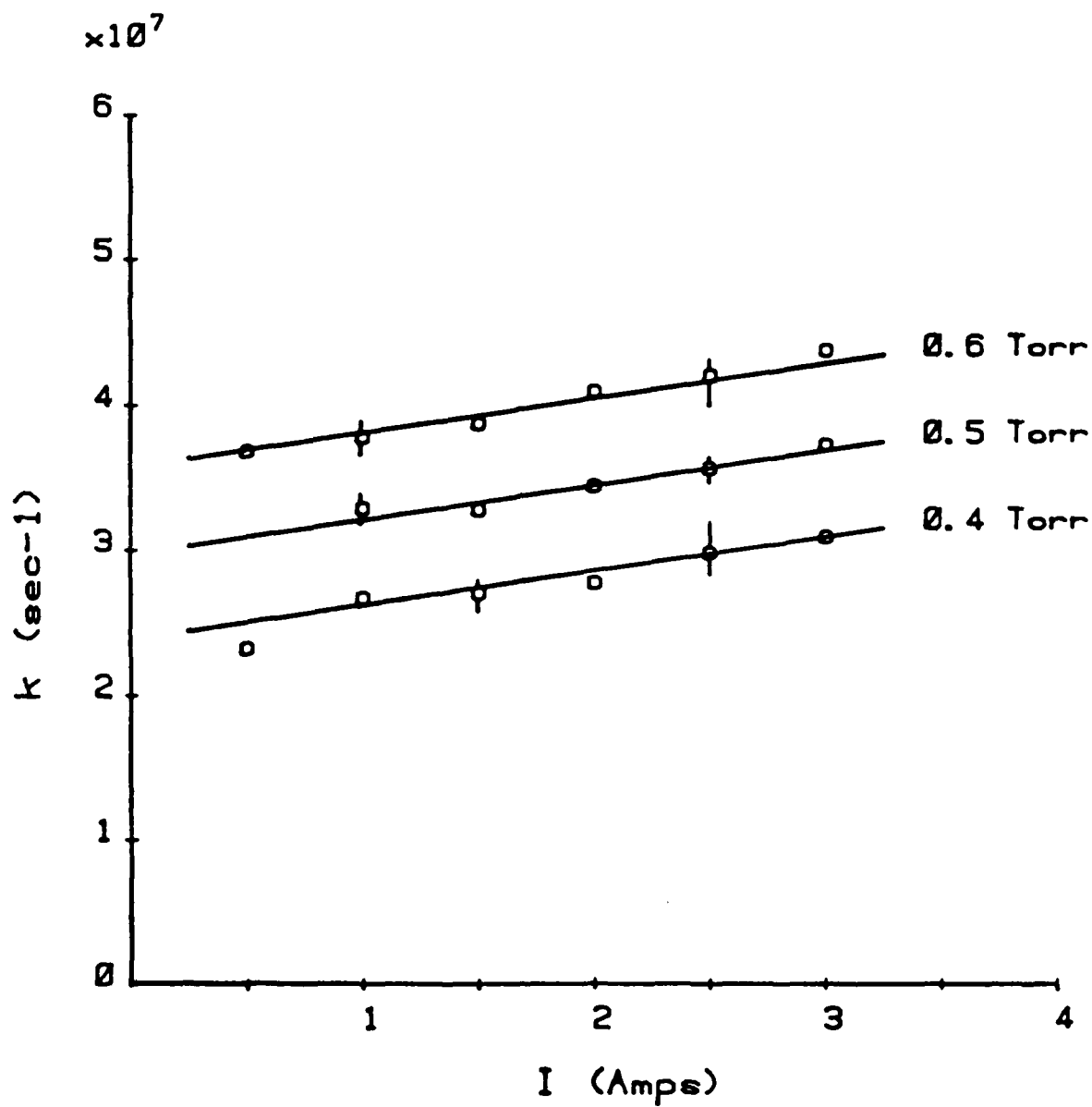


Figure 4. Measured and calculated reciprocal decay constants for $v = 0$, $N = 1$ levels of the $\text{H}_2(\text{c}^3\Pi_u)$ state vs discharge current for various pressures.

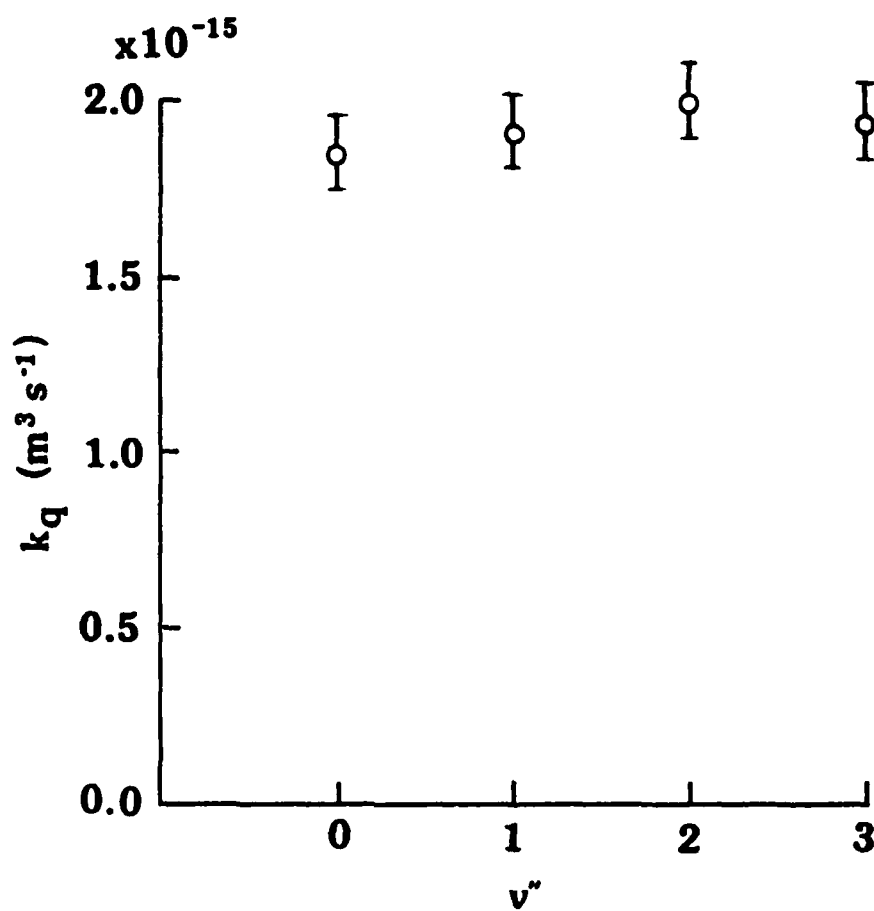


Figure 5. Measured destruction rate coefficients vs vibrational quantum number for $N = 1$ levels of $\text{H}_2(\text{c}^3\Pi_u)$ state.

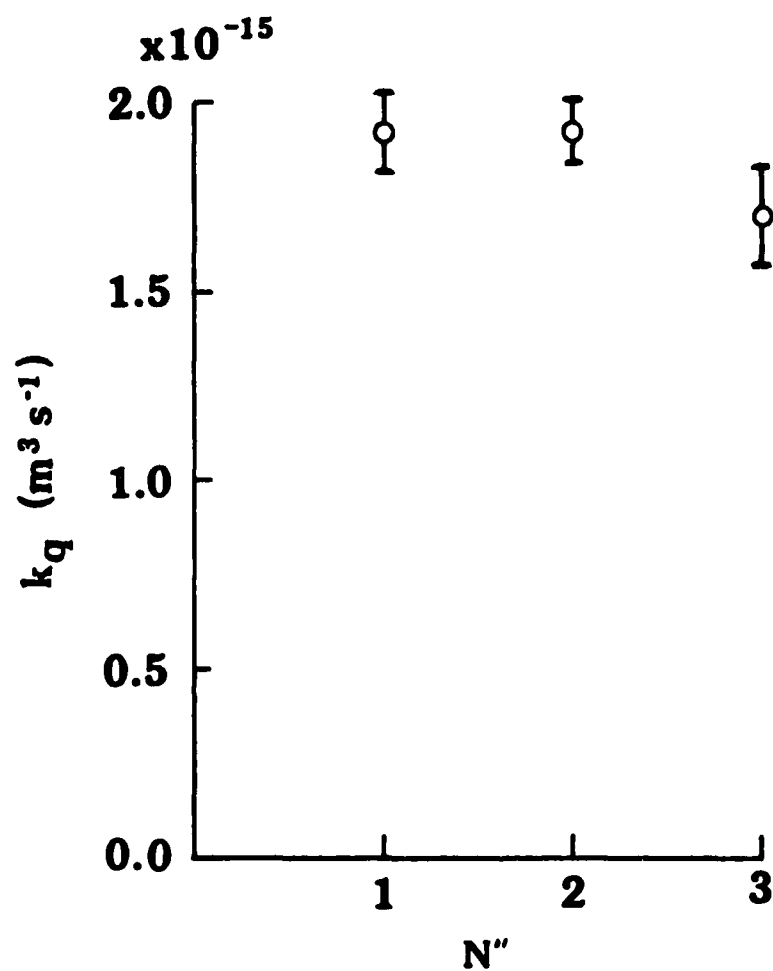


Figure 6. Measured destruction rate coefficients vs rotational quantum number for $v = 1$ levels of $\text{H}_2(\text{c}^3\Pi_u)$ state.

Table I.

Measured rate coefficients for collisional
destruction of vibrational and rotational
levels of $\text{H}_2(\text{c}^3\Pi_u)$ metastables

Vibrational level	Rotational level	Rate coefficient
v	N	$(10^{-15} \text{ m}^3 \text{ s}^{-1})$
0	1	1.85 ± 0.11
1	1	1.91 ± 0.10
1	2	1.92 ± 0.08
1	3	1.70 ± 0.12
2	1	1.98 ± 0.10
3	1	1.93 ± 0.10

Table II.

Levels examined in search for collisional coupling
between $C^3\Pi_u$ and $a^3\Sigma_g^+$ states of H_2

N	v	λ (nm)	N	v	λ (nm)	Signal observed
$C^3\Pi_u$ (depleted)			$a^3\Sigma_g^+$ (observed)			
1	1	588.82	1	1	608.08	yes*
1	0	593.14	1	0	601.83	yes*
1	0	593.14	1	1	608.08	no
2	0	596.35	1	0	601.83	no
$C^3\Pi$ (depleted)			$C^3\Pi$ (observed)			
1	1	602.13	3	1	588.39	no

*The observation of a signal does not necessarily mean that
collisional coupling was responsible. See text.

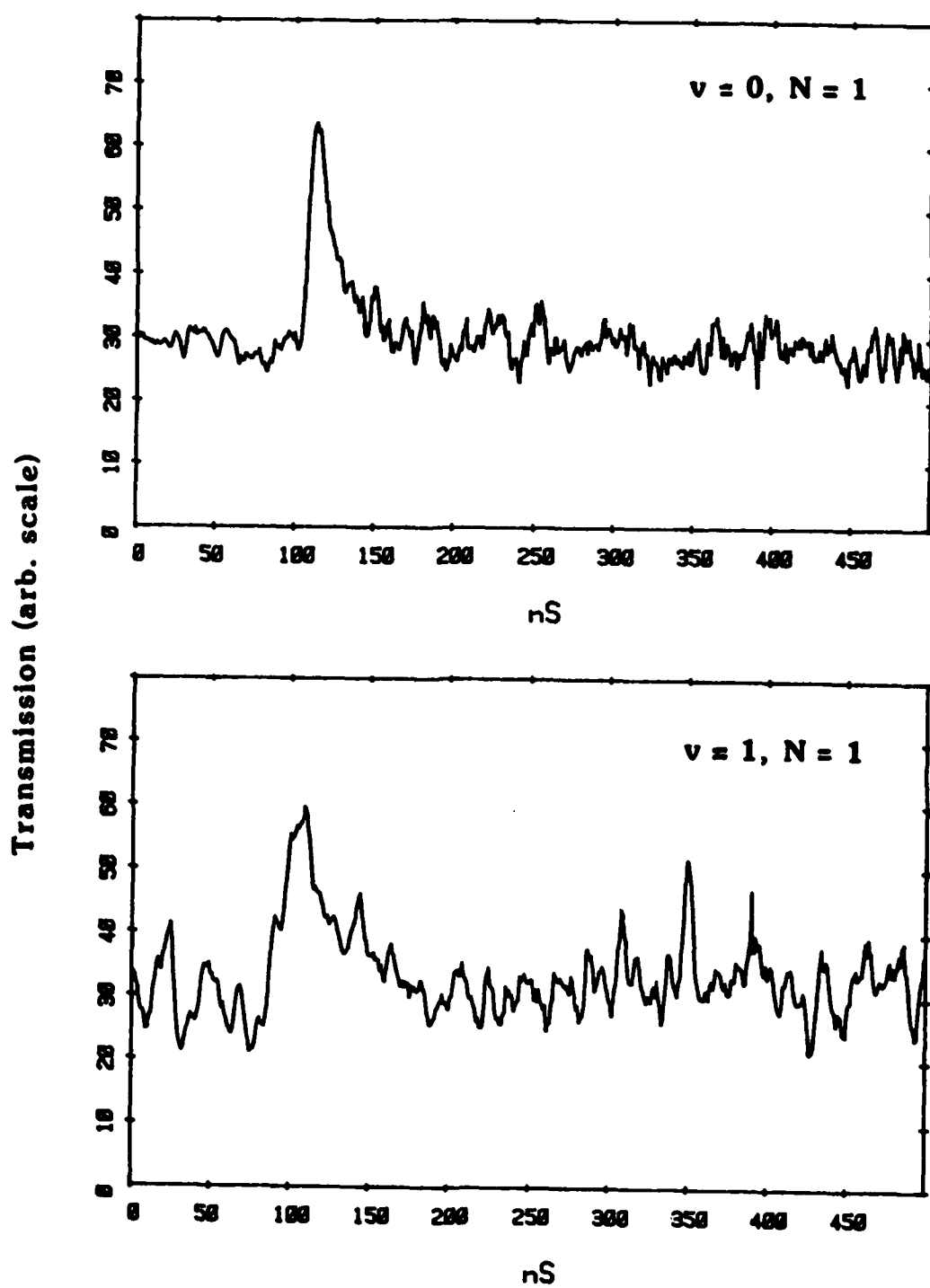


Figure 7. Absorption transients for $v = 1, N = 1$ level (top) and $v = 0, N = 1$ level (bottom) of $a^3\Sigma_g^+$ state resulting from laser induced depletion of the corresponding levels of the $c^3\Pi_u$ state.

$v = 0$, $N = 1$ level of the $a^3\Sigma_g^+$ state when the corresponding levels of the $c^3\Pi_u$ state were depleted with the pulsed laser. As indicated in Table II, no other signals indicative of collisional coupling were detected that were above the relatively high noise level resulting from the short radiative lifetime for the $a^3\Sigma_g^+$ state.² We have not completed our analysis of these waveforms. Only that for the $v = 1$, $N = 1$ level has the expected time dependence, i.e., a relatively slow decrease of a state population and a recovery in a time comparable with that for the $c^3\Pi_u$ levels. Since the waveform for the $v = 0$, $N = 1$ level resembles those for the $c^3\Pi_u$ levels, further tests for proper line identification are necessary before final conclusions can be reached. Table II also shows that for the $v = 1$ levels of the $c^3\Pi_u$ state we did not observe a decrease in the density of the $N = 3$ level when the $N = 1$ level population was depleted with the pulsed laser. This observation suggests that collisions resulting in changes of N by 2 are not probable. Changes of N by 1 with the expected absence of change of ortho-para symmetry would be difficult to detect, since the final level predissociates rapidly ($\sim 10^{-9}$ s). These observations are consistent with our expectation that the quenching of the $c^3\Pi_u$ metastables is too rapid to be accounted for by rotational excitation.

SECTION III

H₂ METASTABLE EXCITATION BY ELECTRONS

The objective of these measurements is to determine the coefficients for the excitation of H₂(c³Π_u) metastables by electrons under discharge conditions. The technique being developed is to combine measurements of the absolute metastable density with our previous measurements of the collisional destruction rate coefficients to calculate the production rate and excitation coefficients. Comparison of these experimental excitation coefficients with theoretical values serves to test proposed excitation cross sections used in modeling discharge devices such as positive and negative ion sources, thyratrons, and plasma processors. Since the work described in this section is new and incomplete, the results cited illustrate the techniques being developed and tested and should not be regarded as final.

The apparatus used in these measurements is the same as that shown in Fig. 2, except that the discharge tube was modified by the addition of two wall probes and a second anode for the differential measurement of electric field strengths and by moving the cathode out of the optical absorption path. The change of the cathode position followed the discovery that significant absorption in the discharge tube of Fig. 2 occurred in the cathode region. A photomultiplier mounted on a moveable platform was added to allow observation of the time and spatial dependence of the light emission while testing for discharge nonuniformities such as striations. The discharge is operated in the pulsed, high current (3 μs long and 1 A current) mode, since attempts to obtain useful absorption without striations using low current dc discharges were unsuccessful. The electric field probes were constructed of 0.08 mm tungsten wire in the form of a ring adjacent to the tube wall so as to

minimize perturbation of the discharge. High voltage oscilloscope probes was used to measure the time dependent floating potentials of the probes. The impedance of the probe circuit was varied to demonstrate lack of significant loading of the plasma by the probe. Figure 8 shows representative discharge current, probe voltages, and absorption transients. We see that the discharge current has reached a plateau by about $1 \mu s$ after the initiation of the discharge. By reading the current, probe voltage differences, and absorption at this time we were able to make measurements before the build up of significant longitudinal spatial variations in the discharge light output and, presumably, before the build up of longitudinal electric field variations.³

The solid points of Fig. 9 show the resultant E/n vs nR data for these pulsed discharges. The solid curve shows the predictions of theory⁴ when the charged particle losses are assumed to be determined by ambipolar diffusion and when the ionization coefficients are calculated using the cross section of Buckman and Phelps.⁵ The open points show the measured E/n vs nR values calculated from the pulsed discharge data of Breusova⁶ and the dc positive column data of Güntherschulze.⁷ On the basis of the current dependence found by Breusova we expect the steady state values of Güntherschulze to be low. Note that our discharge pulse lengths are much shorter than those of Breusova so that we can operate at higher currents than those at which she found significant heating effects. Although the agreement in magnitude between our experimental results and theory is good, the variation of the experimental E/n with nR is too slow at the larger nR values. This divergence may be associated with the greater tendency for striations to develop at the higher gas densities.

A key part of this experiment is the measurement of the absolute fractional absorption from which one can determine the absolute metastable

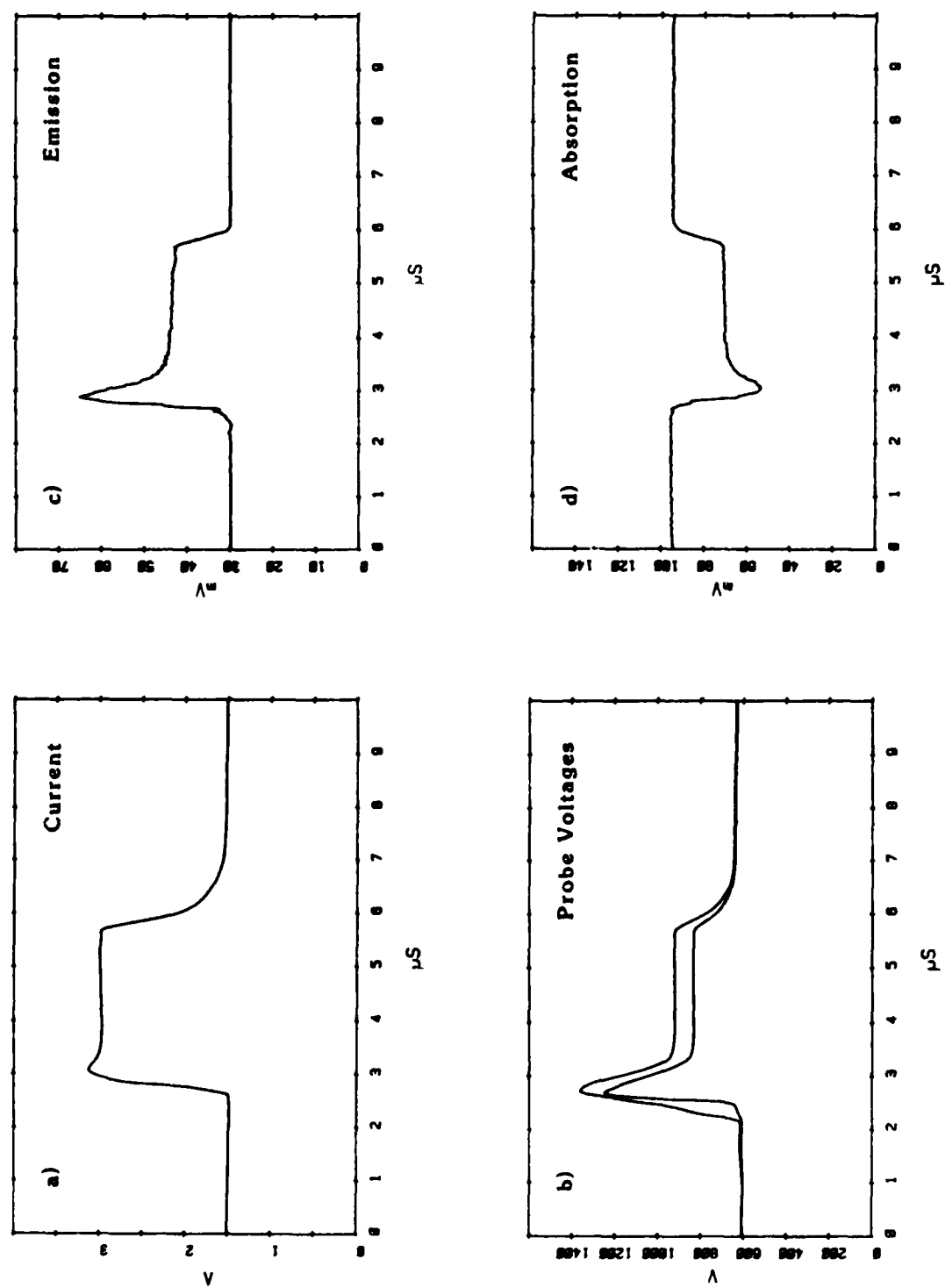


Figure 8. Representative current, probe voltages, emission and absorption traces for discharge in H_2 .

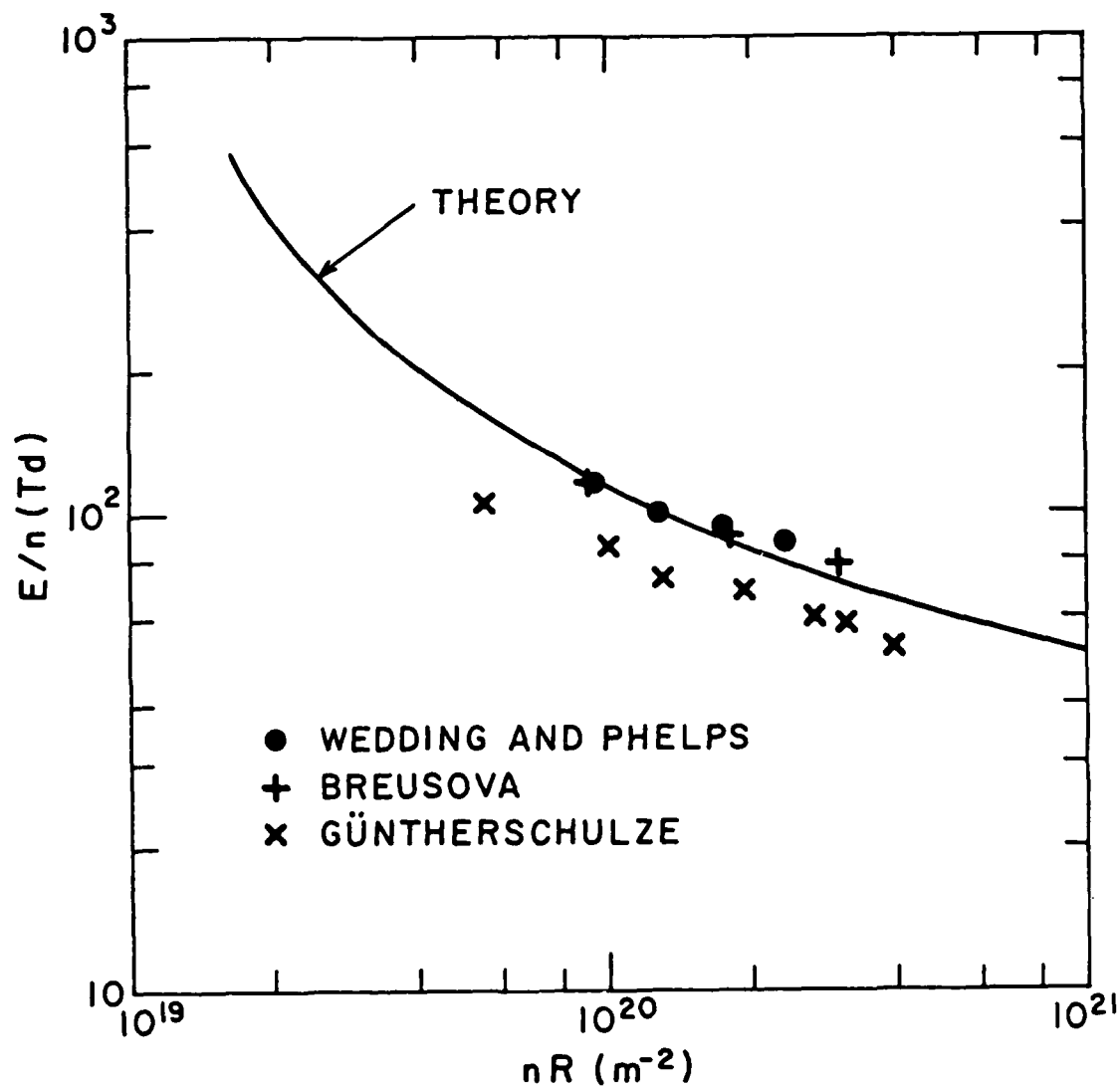


Figure 9. Electric field to gas density ratio E/n for pulsed discharges in H_2 . The solid points are our experimental data, while the + and x are those of Breusova and of Güntherschulze, respectively. The line is calculated from ambipolar diffusion theory and theoretical ionization coefficients.

density. These measurements are made using the single mode dye laser apparatus and technique which we developed previously for the measurement of rare gas metastable densities.^{8,9} Figure 10 shows a measured absorption line profile for the 588.8 nm line caused by transitions from the $v = 1, N = 1$ level of the $c^3\Pi_u$ state to the $v = 1, N = 1$ level of the $i^3\Pi_g$ state. Immediately apparent is the fine structure splitting of about 6 GHz for the $c^3\Pi_g$ state.¹⁰ Somewhat bothersome is the apparent excess absorption between the fine structure components. Further tests of such line profiles are necessary. In order to obtain absolute $c^3\Pi_u$ level densities it is necessary to know the radiative transition probability for this line. At present the only data available is the radiative lifetime for the upper state of the transition.¹¹ The radiative branching ratio for transitions from the $i^3\Pi_g$ state to the levels of the $c^3\Pi_u$ state relative to the repulsive $b^3\Sigma_u^+$ state are unknown. In the absence of such data, one use of our results will be the determination of this branching ratio. Fortunately, efforts are underway elsewhere¹² to calculate radiative transition probabilities for the triplet system of H_2 .

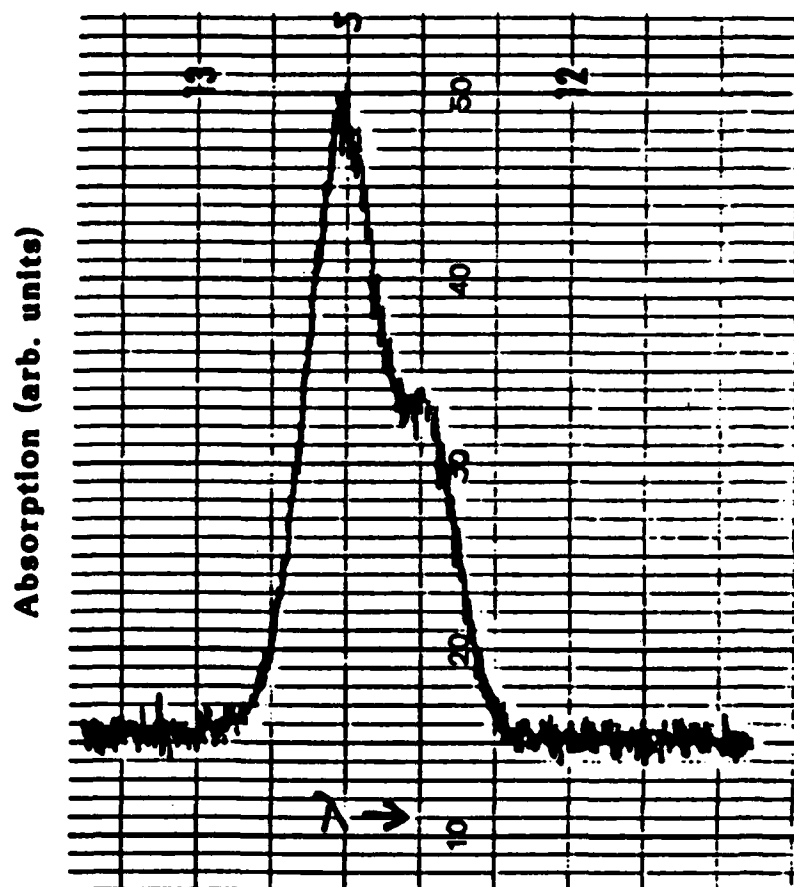


Figure 10. Absorption line profile for the $\text{H}_2(\text{c}^3\Pi_u, v = 1, N = 1)$ to $\text{i}^3\Pi_g, v = 1, N = 1$ transition at 588.8 nm for a pulsed discharge in H_2 at 1 A current and 1 torr pressure of H_2 .

SECTION IV

MODELS OF $O_2(a^1\Delta_g)$ IN DISCHARGES

In this section we summarize the current state of our attempts to model the observed behavior of $O_2(a^1\Delta_g)$ metastables in pulsed O_2 discharges. The experimental data which we have used for comparison is that of Vasileva et al.¹³ for a short pulsed discharge in Ar- O_2 mixtures. These authors report the relative intensities of both the 1.27 μ m emission from the metastables and the 634 nm emission resulting from collision of pairs of metastables as a function of O_2 concentration in the mixture. More useful to us is the observation of the relative time dependence of the 634 nm dimole emission.

The first step in this project was to update our cross section sets for electrons in O_2 and in Ar. This update resulted in a set of cross sections for O_2 which are much more consistent with the electron beam data at electron energies above about 20 eV than are the cross sections assembled in 1976 and circulated in JILA Information Center Report No. 28. The changes resulted in negligible change in the low energy discrepancies pointed out in our 1976 work.¹⁴ The update of the Ar cross sections at energies near excitation threshold was based primarily on the recently published swarm experiment and analysis of Tachibana.⁹ At higher energies we made use of theory and electron beam experiments. As measured by Tachibana, the cross sections result in much lower excitation rates for Ar metastables than do previous cross section sets.

The second step was the acquisition and adaptation to our problem of a chemical kinetics code from the Chemical Kinetics Division of NBS.¹⁵ Next a set of rate coefficients for the electron excitation and excited state reactions of interest was assembled. The electron excitation and ionization

rate coefficients for 20% O_2 in Ar are shown in Fig. 11, while the excited state reaction rate coefficients are listed in Table III.

Figure 12 shows comparisons of the relative experimental 634 nm emission data of Vasileva et al. (solid curve) with our calculations of the square of the $O_2(a^1\Delta_g)$ metastable density for several different assumptions as to the pulsed discharge conditions. The dashed curves from our model are labeled with atomic oxygen density and the $O_2(a^1\Delta_g)$ density at the beginning of the afterglow. We note that dashed curve labeled 1.2×10^{22} , 2.6×10^{21} , which are the O and $O_2(a^1\Delta_g)$ densities calculated with our electron excitation rate coefficients, shows no maximum such as found experimentally. The other dashed curves show the afterglow calculations when it is assumed that no $O_2(a^1\Delta_g)$ metastables are present at the end of the discharge and the atomic O density is varied. None of the initial conditions shown reproduce the time behavior of the observed 634 nm emission. It would appear that much larger quenching rate coefficients for the $O_2(a^1\Delta_g)$ metastables or much larger net recombination rates for O atoms are required. Perhaps the temperature rise of about a factor of two during the afterglow is important.

An additional problem with our model is that the efficiency of conversion of O atoms into $a^1\Delta_g$ molecules is low, e.g., about 2%, for conditions corresponding to the discharge energy input in the experiments of Vasileva et al. On the other hand, if one assumes that all of the input discharge energy is used to dissociate O_2 , the calculated O atom density is equal to the $a^1\Delta_g$ density which these authors claim to be present in the afterglow of their discharge. Some critical reactions in determining the efficiency of metastable formation are the three body formation of O_3 involving two O_2 molecules and the destruction¹⁶ of O_3 by O. If both of these reactions lead to the formation of $a^1\Delta_g$ metastables, one begins to approach the efficiency

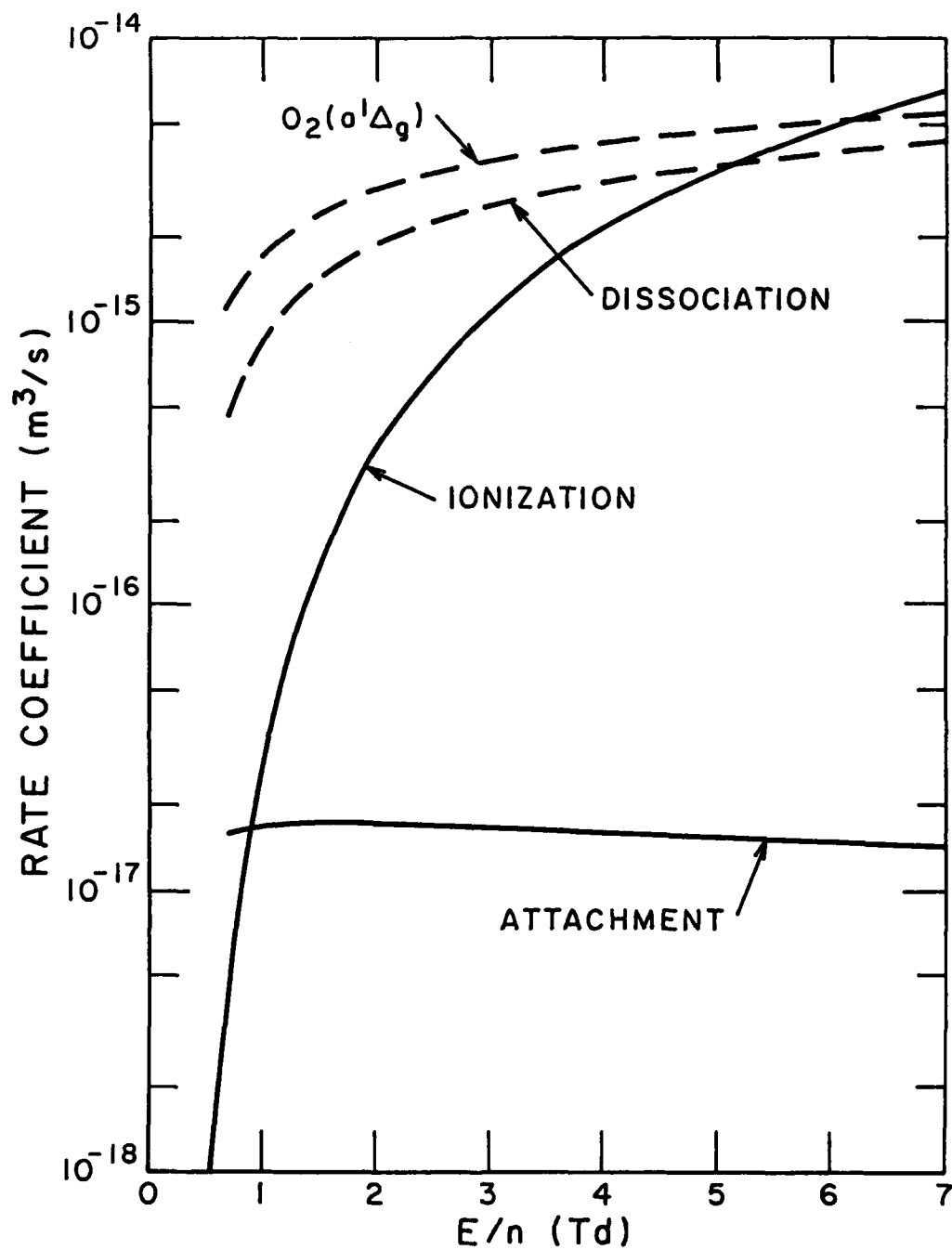


Figure 11. Electron dissociation, ionization, and metastable excitation coefficients for 33% O₂ in Ar vs E/n as calculated from our revised electron cross section sets.

Table III

Reactions in afterglow of O₂-Ar discharge at 300 K.

Reaction	Rate coefficient	Reference
$e + O_2 + O_2 \rightarrow O_2^- + O_2$	$3 \times 10^{-42} \text{ m}^6/\text{s}$	L. M. Chanin, A. V. Phelps and M. A. Biondi, Phys. Rev. <u>128</u> , 219 (1962).
$e + O_2 + Ar \rightarrow O_2^- + Ar$	$5 \times 10^{-44} \text{ m}^6/\text{s}$	H. Shimamori and Y. Hatano, Chem. Phys. <u>21</u> , 187 (1977).
$e + O_2(a) + O_2 \rightarrow e$	$1 \times 10^{-15} \text{ m}^3/\text{s}$	Calc. from cross sections in JILA Information Center Report 28, A. V. Phelps, Sept. 1985.
$e + O_2^+ + 2O$	$2 \times 10^{-13} \text{ m}^3/\text{s}$	E. Alge, N. G. Adams and D. Smith, J. Phys. B. <u>16</u> , 1433 (1983).
$O_2^- + O + O_3 \rightarrow e$	$5 \times 10^{-16} \text{ m}^3/\text{s}$	D. L. Albritton, Atomic and Nuclear Data Tables <u>22</u> , 1 (1978).
$O^- + O + O_2 \rightarrow e$	$1.9 \times 10^{-16} \text{ m}^3/\text{s}$	F. C. Fehsenfeld, in Interactions between Ions and Molecules, ed. by P. Ausloos (Plenum, New York, 1975), p. 387.
$O_2^- + O_2^+ + 2O_2$	$4 \times 10^{-13} \text{ m}^3/\text{s}$	J. T. Moseley, R. E. Olson and J. R. Peterson, Case Studies in Atomic Physics, <u>5</u> , 1 (1975).
$O^- + O_2^+ + O + O_2$	$1 \times 10^{-13} \text{ m}^3/\text{s}$	J. T. Moseley, R. E. Olson and J. R. Peterson, op. cit.
$O + O + O_2 \rightarrow O_2(a) + O_2$	$1.5 \times 10^{-45} \text{ m}^6/\text{s}$	T. Baurer and M. H. Bortner, in DNA Reaction Rate Handbook, ed. by M. H. Bortner and T. Baurer, (General Electric, Philadelphia, 1979), Chap. 24.
$O + O + Ar \rightarrow O_2(a) + O_2$	$1 \times 10^{-46} \text{ m}^6/\text{s}$	D. W. Trainor, D. O. Ham and P. Kaufman, J. Chem. Phys. <u>58</u> , 4599 (1973).
$O + O_2 + O_2 \rightarrow O_3 + O_2$	$6.2 \times 10^{-46} \text{ m}^6/\text{s}$	D. L. Baulch et al., J. Chem. Phys. Ref. Data <u>13</u> , 1259 (1984).
$O + O_2 + Ar \rightarrow O_3 + Ar$	$3.5 \times 10^{-46} \text{ m}^6/\text{s}$	R. V. Donovan, D. Husain and L. J. Kirsch, Trans. Faraday Soc. <u>66</u> , 2551 (1970).
$O_3 + O + 2O_2$	$8 \times 10^{-21} \text{ m}^3/\text{s}$	D. L. Baulch, op. cit.
$O_2(a) + O_2 \rightarrow 2O_2$	$2.2 \times 10^{-21} \text{ m}^3/\text{s}$	D. L. Baulch, op. cit.
$O_2(a) + Ar \rightarrow O_2 + Ar$	$9 \times 10^{-27} \text{ m}^3/\text{s}$	R. J. Collins, D. Husain, and R. J. Donovan, Faraday Trans. II, <u>69</u> , 145 (1973).
$O_2(a) + O + O_2 \rightarrow O$	$1 \times 10^{-22} \text{ m}^3/\text{s}$	Our estimate
$O_2(a) + O_2(a) \rightarrow O_2(a) + O_2$	$3 \times 10^{-23} \text{ m}^3/\text{s}$	R. G. Derwent and B. A. Thrush, Faraday Soc. Trans. <u>67</u> , 2036 (1971); V. Schurath, J. Photochem. <u>4</u> , 215 (1975).
$Ar^H + O_2 \rightarrow Ar + 2O$	$2 \times 10^{-16} \text{ m}^3/\text{s}$	J. E. Velasco, J. H. Klotz, and D. W. Setser, J. Chem. Phys. <u>69</u> , 4357 (1973).
$O_2(a) + O_3 \rightarrow 2O_2 + O$	$4 \times 10^{-21} \text{ m}^3/\text{s}$	D. L. Baulch et al., op. cit.
$O_2(a) + h\nu \rightarrow O_2$	$2.6 \times 10^{-4} \text{ s}^{-1}$	R. M. Badger, A. C. Wright, and R. F. Whitlock, J. Chem. Phys. <u>43</u> , 4345 (1965).
$O_2(a) + O_2(a) \rightarrow 2O_2 + h\nu$	$5.5 \times 10^{-29} \text{ m}^3/\text{s}$	P. Borrell and N. H. Rich, Chem. Phys. Lett. <u>99</u> , 144 (1983).

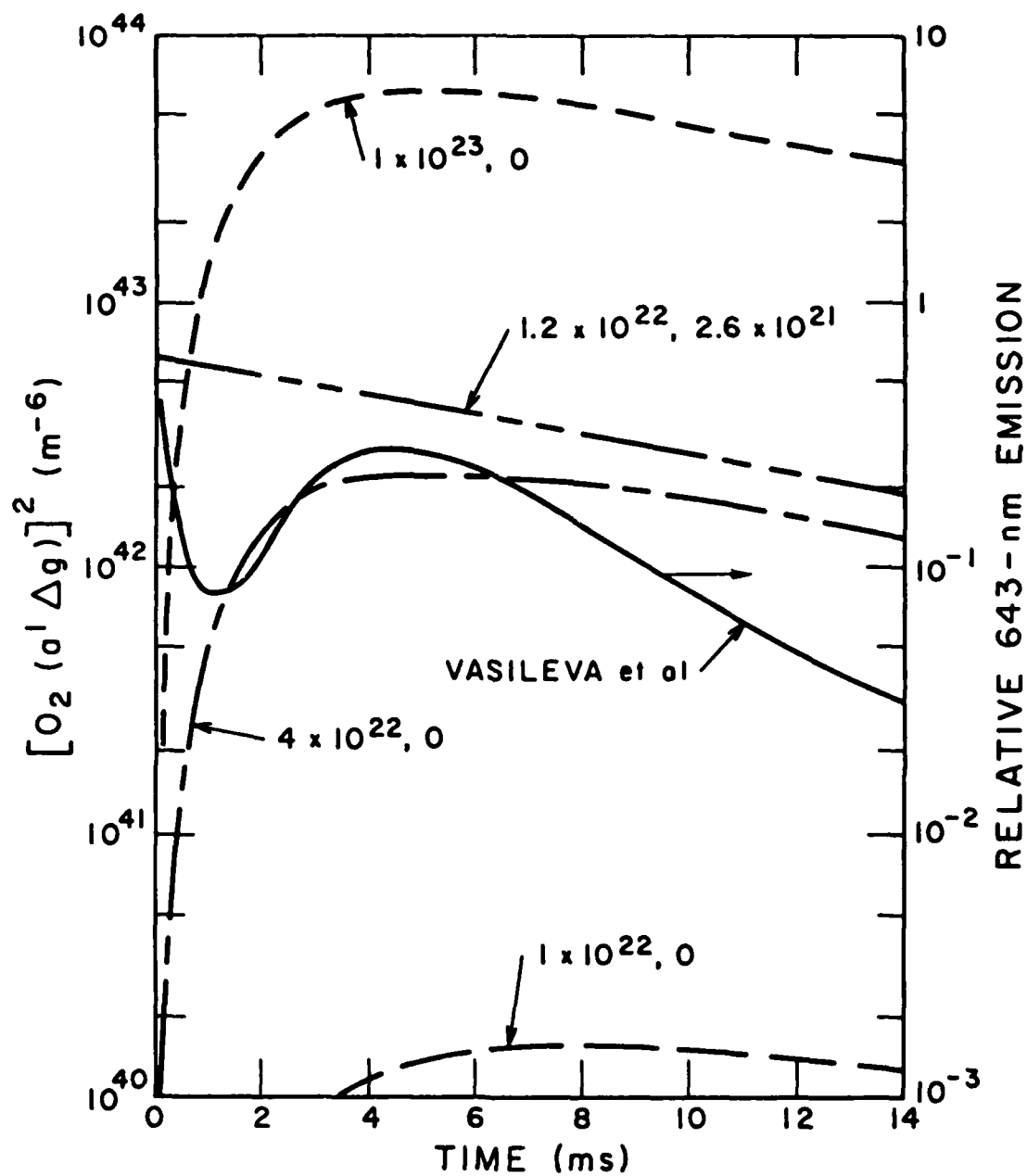


Figure 12. Comparison of measured relative 634 nm emission data with the calculated square of the $O_2(a^1\Delta_g)$ density for a 33% O_2 = 67% Ar mixture. The solid curve is taken from the experimental data of Vasileva et al., while the dashed curves are from the model discussed in the text.

required. Both of the reactions are energetically allowed, but the former would have very little excess energy.

We conclude that our model is in serious disagreement with the results of Vasileva et al. and that the required modifications are not obvious. In view of the importance of competition between O_3 formation and $a^1\Delta_g$ formation, it would be very desirable to have simultaneous measurements of these densities.

SECTION V

CONCLUSIONS

The results described in this report show that all of the metastable levels of the $c^3\Pi_u$ state of H_2 are rapidly destroyed in collisions with H_2 under electrical discharge conditions. As a result the populations of the metastable levels are expected to be only marginally larger than those of nearby radiating levels, rather than much larger as suggested in some previous models of these discharges. Furthermore, our preliminary measurements of electric field strengths in the positive column of pulsed H_2 discharges show that when the energy input per molecule is small the E/n values required to maintain the steady state discharge are very close to values predicted using our recently recommended electron collision cross section set. The apparent success of our techniques for electric field and metastable absorption measurements at low energy input densities suggests future measurements at higher energy densities in an effort to define the role of vibrationally excited H_2 in these discharges.

The analysis of the behavior of the $O_2(a^1\Delta_g)$ metastables in O_2 -Ar has shown that there is a serious deficiency in our model. We are unable to simulate the maxima in the 634 nm emission produced by $O_2(a^1\Delta_g)$ metastables as observed by Vasileva et al. Until this problem is solved there does not seem much point in pursuing this modeling.

In view of the success of the laser diagnostic techniques in the measurement of the collisional destruction rate coefficients for the $H_2(c^3\Pi_u)$ metastable, we recommend that these techniques be applied to measurements of the collisional quenching and electron excitation of the higher metastable states of N_2 , i.e., the $a''^1\Sigma_g^+$ and $a'^1\Sigma_u^-$ states. These states have been

the subject of much discussion in recent years because of their possible importance in multi-step ionization processes in N_2 discharges and shock waves.

REFERENCES

1. H. Tischer and A. V. Phelps, Chem. Phys. Lett. 117, 550 (1985).
2. K. A. Mohamed and G. C. King, J. Phys. B 12, 2809 (1979).
3. A. Garscadden, in Gaseous Electronics, Electrical Discharges, edited by M. Hirsch and H. J. Oskam (Academic, New York, 1978), Vol. 1, p. 65.
4. C. H. Muller, III and A. V. Phelps, J. Appl. Phys. 51, 6141 (1980).
5. S. J. Buckman and A. V. Phelps, J. Chem. Phys. 82, 4999 (1985).
6. L. N. Breusova, Zhur. Tekh. Fiz. 39, 862 (1969) [Sov. Phys. — Techn. Phys. 14, 862 (1969)].
7. A. Guntherschulze, Z. Physik 42, 718 (1927).
8. K. Tachibana and A. V. Phelps, Bull. Am. Phys. Soc. 26, 714 (1981).
9. K. Tachibana, Phys. Rev. A 34, 1007 (1986).
10. W. Lichten, T. Wik, and T. A. Miller, J. Chem. Phys. 71, 2441 (1979).
11. E. E. Eyler and F. M. Pipkin, Phys. Rev. Lett. 47, 1270 (1981) and J. Chem. Phys. 77, 5315 (1982).
12. T. L. Kwok, S. Guberman, A. Dalgarno, and A. Posen, preprint (1986).
13. A. Vasileva, I. A. Grishina, K. S. Klopovskii, A. S. Kovalev, A. P. Osipov, A. T. Rakhimov, and T. V. Rakhimova, Fiz. Plasmy 11, 221 (1985) [Sov. J. Plasma Phys. 11, 130 (1985)].
14. S. A. Lawton and A. V. Phelps, J. Chem. Phys. 69, 1055 (1978).
15. R. L. Brown, HICHM: A Fortran Code for Homogeneous Isothermal Chemical Kinetics Systems, NBSIR 81-2281 (unpublished).

END

7-87

DTIC